ELSEVIER

Journal of Structural Geology xx (xxxx) 1–13

JOURNAL OF STRUCTURAL GEOLOGY

www.elsevier.com/locate/jsg

Late Pliocene–Pleistocene stress field in the Teruel and Jiloca grabens (eastern Spain): contribution of a new method of stress inversion

L.E. Arlegui[a,*], J.L. Simón[a], R.J. Lisle[b], T. Orife[b,1]

[a]*Departamento de Geología, Universidad de Zaragoza, Spain*
[b]*Laboratory for Strain Analysis, School of Earth, Ocean and Planetary Sciences, Cardiff University, UK*

Received 17 June 2004; received in revised form 8 October 2004; accepted 9 October 2004

Abstract

Samples of non-striated fracture surfaces within clastic materials of Late Pliocene–Pleistocene age from the Teruel grabens (eastern Spain) have been analysed using a stress inversion method based on observations of slip sense. The results obtained at 21 sites are compared with Late Miocene–Early Pliocene extensional stress tensors previously inferred from striated faults in the same area. The similarity between both sets of stress states suggests that the extensional Miocene–Pliocene stress field essentially continues (with minor changes) into Pliocene–Pleistocene times. The main changes involve (a) the dominant trend of σ_3 trajectories, which evolve from ESE to ENE; (b) the waning of the compressional component caused by Europe–Iberia–Africa convergence; and (c) the progressive trend towards a multidirectional extension regime. Stress deflection caused by large-scale extensional faults as well as switching of σ_2 and σ_3 axes induced by fracture development are common within this stress field. They produce groups of local stress ellipsoids with σ_3 axes orthogonal to each other and either orthogonal or parallel to the faults bounding the grabens. The regional consistency of the new results gives support to the new inversion method and demonstrates its utility in research on young sedimentary rocks, where 'gaps' in palaeostress records may exist due to absence of striated faults.

Keywords: Stress inversion; Iberian Chain; Neotectonics; Fault

1. Introduction

The vast majority of palaeostress inversion methods are based on the assumption that the slip direction on each fault in a rock mass is parallel to the maximum resolved shear stress on the fault plane. Bott's equation (Bott, 1959) expresses how the direction of the shear component of stress on a plane relates to the plane's orientation with respect to the stress axes and to the stress ratio. The stress ratio describes the relative values of the principal stresses and hence the overall shape of the stress ellipsoid. Many inversion methods use this equation to address the inverse problem of estimating the stress axes orientations and stress ratio given the observed shear (in the form of striations) on the fault planes (Carey and Brunier, 1974; Carey, 1976, 1979; Armijo and Cisternas, 1978; Etchecopar et al., 1981; Angelier and Bergerat, 1982; Armijo et al., 1982; Simón, 1982, 1986; Etchecopar, 1984; Angelier, 1991; Fry, 1992; Delvaux et al., 1992; Delvaux, 1994; Stapel and Moeys, 1994). There are a variety of other methods that utilise the slip direction to constrain the possible orientations of the principal stresses, e.g. Right Dihedra Method (Pegoraro, 1972; Angelier and Mechler, 1977) and Right Trihedra Method (Lisle, 1987, 1988). However, as with the methods based on the Bott equation, they all require knowledge of the slip direction.

NE Spain has been extensively investigated in terms of palaeostress during the last two decades (Simón, 1982, 1986, 1989; Amigó, 1986; Guimerà, 1988; Casas et al., 1992; Arlegui, 1996; Casas and Maestro, 1996; Arlegui and Simón, 1998; Cortés, 1999). Recently, Liesa (2000) compiled more than 1600 stress inversion results from diverse authors obtained with several methods, with affected rocks spanning from Palaeozoic to Tertiary, representing both compressive and extensional stress fields. The

* Corresponding author. Tel.: +34 976 76 21 27; fax: +34 976 76 11 06
E-mail address: arlegui@unizar.es (L.E. Arlegui).
[1] Now at: BG Group, Reading, UK

0191-8141/$ - see front matter © 2005 Published by Elsevier Ltd.
doi:10.1016/j.jsg.2004.10.013

successive stages of Alpine rifting and compression have been characterised with particular detail along the Iberian Chain. However, a cursory look at the published data reveals obvious gaps in the palaeostress record, such as the lack of results from recent deposits and soft rocks. In both cases, the main problem is the paucity, due to the physical properties of the wall rocks, of striated fault surfaces over limited areas that most stress inversion methods require for analysis. Current strategies for overcoming the problems of detecting slip direction from faults in young (unlithified) sediments where striation are lacking include the use of scanning electron microscope (SEM) images of fault surfaces and stress inversions based solely on observations of dip separation (Lisle et al., 2001).

Our purpose in this paper is to explore the possibilities that the Lisle et al. (2001) method offers for stress inversion of fractures measured in recent (Upper Pliocene and Pleistocene), mainly clastic materials. The application of the method to the Teruel and Jiloca grabens allows the comparison of our results with older (Late Miocene–early Pliocene) stress tensors previously inferred in the same area.

2. Methodology of stress inversion based on fault slip sense

Lisle et al. (2001) explore the possibility of stress tensor estimation from fault slip sense alone. They show that knowledge of the sense of the dip-slip component on a fault with dip angle γ indicates the sign of gradient of normal stress $\delta\sigma/\delta\gamma$. Such information, if available for fault planes with a range of orientation, allows the orientation of principal stress axes to be constrained. Their approach involves a comparison of the levels of normal stress calculated for the observed fault with that calculated on a slightly steeper-dipping imaginary fault plane. In order to test the validity of their inversion results, they have used artificial data samples as well as natural samples in which slip lineations were not taken into account, which allows comparison with the results of conventional analysis based on striated faults. In common with other methods of stress inversion, the authors suggest that data sample size, a preferred orientation of faults or poly-phase deformation will affect the reliability of stress results.

The grid search method of inversion proposed by Lisle et al. (2001) is based on a computer search for stress tensors compatible with the observed faults and their respective slip senses. The search involves the definition of a 4-D solution space that is systematically explored by varying the orientations of σ_1, σ_2, σ_3 and the value of stress ratio Φ. The grid or mesh is the interval between two consecutive trial stress tensors. The precision of such stress inversion strategy is therefore a function of the grid search parameters. The number of observed slip senses that match the predicted slip senses is the criterion for expressing the goodness-of-fit of the trial stress tensors.

In comparison with the fault slip inversion strategies that utilise the knowledge of the orientation of slickenlines on faults, the procedure proposed by Lisle et al. (2001) produces a wider range of compatible stress tensor solutions. This increased range of compatible stress tensor solutions is a consequence of the 'reduced information content' of slip sense data when it is compared with slip vector data. Lisle et al. (2001) report that the precision of the method and its ability to recognise mixed data sets (potentially sourced from poly-phase deformation) are improved as sample size is increased.

Orife et al. (2002) detail a computer algorithm to implement the stress inversion procedure of Lisle et al. (2001). These authors prefer to present the inversion results using stereoplots that show modal solutions of the respective stress axes and a frequency histogram of the stress ratio values for displaying compatible stress tensors.

Lisle et al. (2001) and Orife et al. (2002), by implication, utilise the orientation of the fault plane as the reference frame for defining a normal/reverse dip-slip movement. A potential limitation of using slip sense data relates to the assumptions regarding the initial orientation of the reference markers that are used to define the sense of a displacement. However, if these reference markers are horizontal or their cut-off lines are horizontal (as they are in the present study area), the sense of separation in the down-dip line of the fault reliably indicates the sense of dip-slip movement.

3. Geological setting

The eastern sector of the Iberian Chain shows a large network of extensional faults with dominant strikes NNE–SSW and NNW–SSE (Fig. 1), which postdate the compressive structures. These faults developed during Neogene times, as the eastern margin of the Iberian Peninsula became dominated by the influence of rifting in the Valencia Trough (Álvaro et al., 1979; Vegas et al., 1979). The two main orientations of faults are inherited from late-Variscan and Mesozoic times, which moved as reverse and strike-slip faults during the Paleogene compression and were again reactivated as normal faults during Neogene and Pleistocene times. The latter gave rise to grabens that were filled with continental deposits. The NNE–SSW-trending Teruel and Maestrazgo grabens are parallel to the Valencia Trough. They represent the onshore deformation of the eastern Iberia Neogene rift (Simón, 1982; Roca and Guimerà, 1992). The Jiloca graben, located west of the former area, shows a NNW–SSE trend probably controlled by S_{Hmax} stress trajectories related to recent intraplate compression (Simón, 1989).

Extension propagated westward from the offshore Valencia Trough (where sedimentary infilling initiated by Early Miocene times), to the Maestrazgo grabens (Early–Middle Miocene), Teruel graben (Late Miocene) and Jiloca graben (Late Pliocene) (Capote et al., 2002). Local

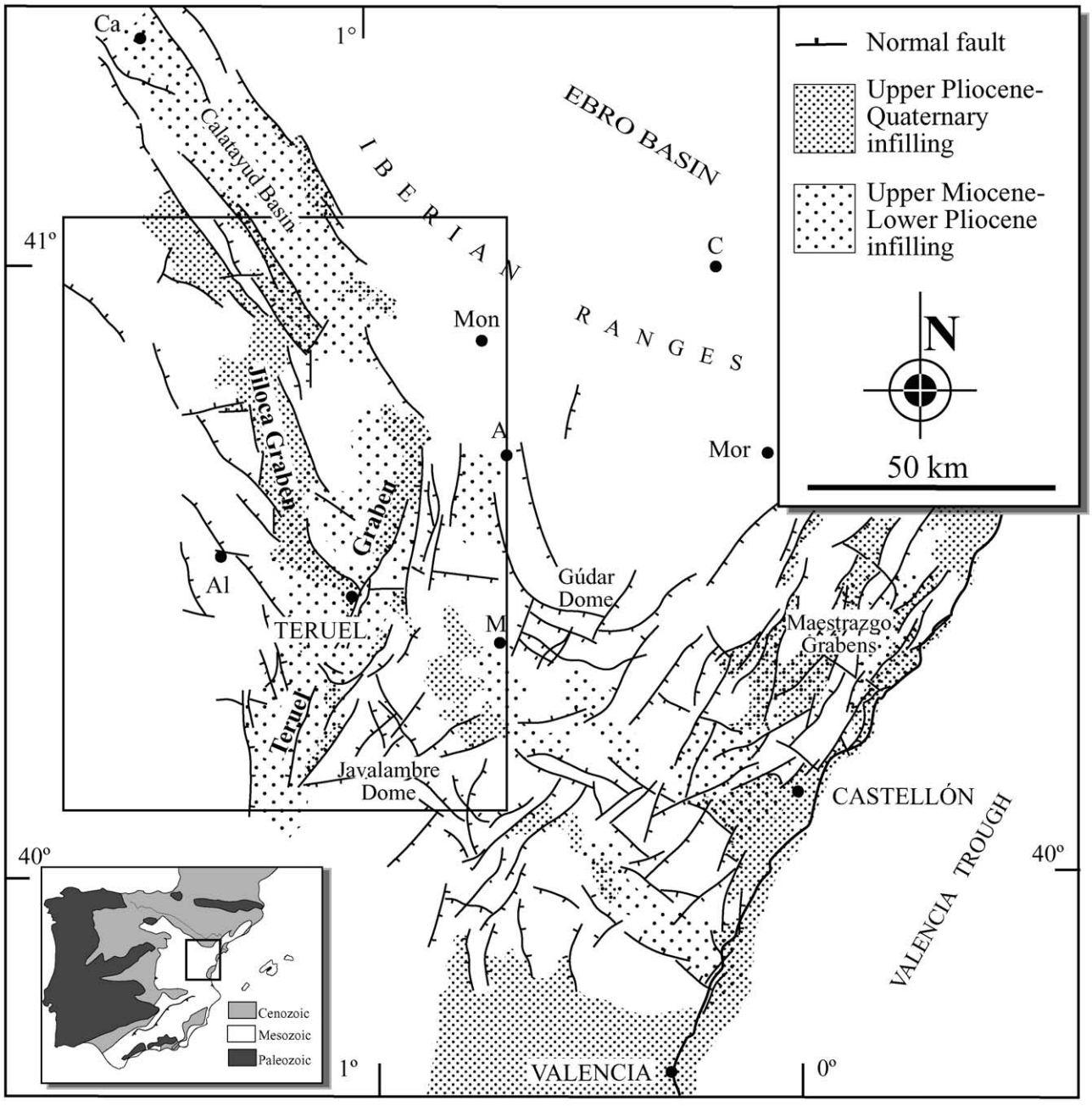

Fig. 1. Schematic map of the Neogene–Quaternary extensional structures in the eastern Iberian Chain, showing the locations of the Teruel and Jiloca grabens. A: Aliaga; Al: Albarracín; C: Calanda; Ca: Calatayud; M: Mora de Rubielos; Mon: Montalbán; Mor: Morella.

reactivation of normal faults also occurred during the Quaternary. By Early Pleistocene times, several NNE–SSW striking faults underwent decametric-scale offsets at the boundaries of the Teruel graben (Simón, 1983; Moissenet, 1985) and, probably, hectometric ones in the eastern Maestrazgo grabens (Simón, 1982). NW–SE striking faults at the eastern limit of the Jiloca graben also show metric to decametric offsets affecting sediments of the Middle and Upper Pleistocene (Capote et al., 1981; Simón and Soriano, 1993).

The evolution of extension can be divided into two main episodes that show differences in stress patterns. The first one (Miocene) produced the main NNE–SSW-trending grabens (Teruel, Maestrazgo), and shows well defined WNW–ESE σ_3 directions as can be inferred from micro- and mesofracture populations (Simón, 1982, 1986; Guimerà, 1988; Liesa, 2000). During the second episode (Pliocene–Pleistocene) the Teruel and Maestrazgo grabens underwent reactivation, while the Jiloca graben was newly created. Faults showing a great variety of strikes moved during that time and large domes (Gúdar and Javalambre massifs; see location in Fig. 1) were developed. Consistent

with this onshore macrostructural pattern, palaeostress analysis performed on striated faults (Simón 1982, 1989; Cortés, 1999; Liesa, 2000) indicate that the stress field was characterised by a near-multidirectional extension regime.

Our work is focused on the Teruel and Jiloca grabens. The Teruel basin is a half-graben (Fig. 2) with its active, eastern boundary controlled by several N–S to NNE–SSW faults (El Pobo, Teruel, Aldehuela, Mas del Olmo, Val de la Sabina faults; see Fig. 1 and map on Fig. 4). It shows a Neogene continental succession reaching up to 400–500 m in thickness and showing sharp lateral and vertical changes. Alluvial fan conglomerates of the basin margin grade both laterally and vertically into mud-flat deposits and lacustrine carbonates and evaporites, composing four main sequences controlled by tectonic subsidence and climate (Anadón and Moissenet, 1996; Alonso and Calvo, 2000). By the Late Pliocene, reactivation of faults and climate changes gave rise to the beginning of the external drainage (Moissenet, 1982; Gutiérrez et al., 1996). This induced sedimentation of new, widespread and relatively homogeneous red clastic deposits that often show pediment morphology. Development of pediments and fluvial terraces continued during Pleistocene, though they cover smaller areas.

The Jiloca graben is a more recent and simple basin showing a narrower sedimentary record. It was the only large structure generated during the Plio-Pleistocene extensional episode. Its precise overall NNW–SSE trend (oblique to the NNE–SSW trend of the grabens previously initiated) results from en-échelon, right releasing arrangement of NW–SE striking faults (Figs. 1 and 4). The largest faults are located at the eastern boundary (Calamocha, Sierra Palomera and Concud faults), the resulting structure usually being an asymmetric graben or even a half-graben (Simón, 1983). Deposits covering the whole basin are Late Pliocene and Pleistocene in age. They mainly include red clastic deposits of small alluvial fans and pediments, their thickness usually reaching only several tens of metres. Miocene–Lower Pliocene lacustrine deposits of the Calatayud and Teruel basins (cut by the Calamocha and Concud faults, respectively) lie unconformably under these red clastic sediments at both the northern and southern terminations of the Jiloca graben, but they are not related to the latter. Carbonate deposits of unknown age, lying between Mesozoic and Plio-Pleistocene clastic deposits, have also been observed in boreholes within the central part of the graben (Rubio, 2004). This keeps open the hypothesis of a small precursor basin in this area, though the development of the entire Jiloca basin was essentially Plio-Pleistocene in time.

Vertical offsets on faults bounding the Teruel and Jiloca grabens can be calculated from changes of elevation registered by stratigraphical and morphological markers. Lacustrine deposits, well dated using the abundant mammal faunas (Adrover, 1986; Alcalá, 1994; Alcalá et al., 2000), have been used for this purpose (IGME, 1983; Moissenet, 1983; Simón, 1983; Cortés, 1999), as well as erosion surfaces and pediment levels (Riba, 1959; Simón, 1982, 1983, 1989; Gracia et al., 1988). The results show hectometric displacements in some cases. The Teruel half-graben has maximum throws approaching 700 m at Sierra del Pobo fault (about 300–350 m during the Miocene, 350–400 m after the Early Pliocene) (Fig. 2). The inferred post-Miocene throw at the Jiloca graben exceed 250 m in the Concud fault, and 175 m the Calamocha fault (though it could be larger in the latter depending upon the interpretation of fault history, since negative inversion and partial erosion of sedimentary infilling could occur during the Miocene). In the case of the Sierra Palomera fault, in the absence of unequivocal stratigraphic markers, a probable value of 400 m is estimated from morphostructural reconstruction (see Fig. 2). Nevertheless, two recent works have proposed alternative models that minimize the magnitude of fault displacements, and attribute the present-day topographic depression to progressive lowering either to successive pediplanation events during Eocene–Miocene compressive uplift (Casas and Cortés, 2002) or to kryptokarstic corrosion in a Pliocene–Quaternary polje (Gracia et al., 2003).

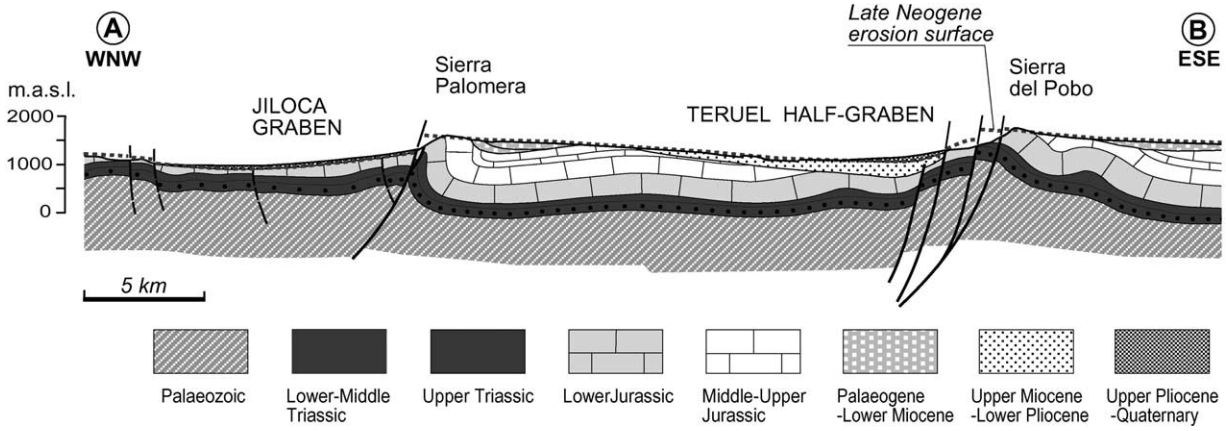

Fig. 2. Cross-section of the Teruel and Jiloca grabens (see location on Fig. 6).

4. Field data and stress results

Palaeostress analysis using the method of Lisle et al. (2001) has been applied to 21 samples of fault planes collected in Upper Pliocene and Pleistocene deposits of the Teruel and Jiloca grabens (see Table 1). Most of the studied outcrops show clastic rocks of continental origin, mainly conglomerate and siltstone deposits formed in alluvial fans and pediments. Other (Pleistocene) sediments correspond to fluvial terraces including gravel, sand, silt or calc tufa. These non-favourable lithologies (soft behaviour, coarse grain-size) and the small lithostatic load (reduced absolute normal stress acting on fracture surfaces) hinder the development of slickenlines indicating directions of fault slip. Whereas, in this region, lacustrine limestones up to the Lower Pliocene have provided numerous samples of striated faults that were analysed using the method proposed by Etchecopar et al. (1981) (Simón, 1989; Cortés, 1999), only one outcrop in clastic Upper Pliocene–Pleistocene sediments has provided a sufficient number of striated faults for palaeostress analysis (Cortés, 1999). This lack of striated fault surfaces enhances the importance of the present work to the knowledge of the recent tectonic evolution of the region.

Five types of fractures were found in the studied outcrops:

(1) Metric to decametric-scale fault surfaces, showing macroscopic (centimetric to metric-scale) offsets; in all cases these show a dip separation with normal sense (Fig. 3a).
(2) Metric-scale fractures with negligible offset on a macroscopic scale, though showing diverse shear indicators (with normal sense in all cases) when observed in close view (Fig. 3b and c): millimetric dip separations; associated minor Riedel fractures (in sand and silt), or rotated pebbles (in unconsolidated gravel).
(3) Metric-scale fractures without any sign of movement, which are interpreted as normal shear fractures (a pure extensional origin is discarded) on the basis of one or more of the following features: smooth surfaces parallel to fractures of types (1) and (2) in the same outcrop; planes making angles with bedding under 75°; conjugate geometry compatible with Andersonian normal faulting (Fig. 3d).
(4) Decimetric to metric-scale pure tensional joints, making angles with bedding of 80–90°, showing irregular surfaces and, in some cases, mineral filling.
(5) Ambiguous fractures with classification as either type (3) or type (4) was not possible from field observation.

A sample containing several tens of fracture planes was collected in each studied outcrop. The sample size was not predetermined, but depended on the density of fractures. Only types (1), (2) and (3) were considered for applying the inversion method of Lisle et al. (2001); they represent about 10, 15 and 75%, respectively, of the analysed data. As the application of the inversion method requires the introduction of slip sense, a normal sense has been attributed to every fracture, even to those of type (3). We interpret that the latter represent shear or hybrid fractures (in the sense of

Table 1
Sites of palaeostress determination with the orientation of inferred stress axes. Reliability assessment: VH: very high; H: high; A: average; L: low

Site	Locality	Lithology	Age	Number of fractures	σ_1	σ_3	Reliability assessment
01	Monreal	Siltstone	Late Pliocene	30	66, 051	20, 266	VH
02	Valdeceladas	Conglomerate	Late Pliocene	27	78, 058	12, 246	A
03	Villarrosano	Siltstone, conglomerate	Late Pliocene	28	Near-vertical	03, 253	H
04	Bco. Ramón	Siltstone, sandstone	Late Pliocene	19	Vertical	00, 065	H
05	Villarquemado	Conglomerate	Late Pliocene	21	Near-vertical	02, 246	A
06	Nevera 1	Conglomerate	Late Pliocene	22	35, 160	30, 355	L
07	Nevera 2	Gravel, silt	Pleistocene	9	Near-vertical	05, 269	A
08	Caudé	Conglomerate	Late Pliocene	25	Vertical	00, 180	H
09	Bco. del Monte	Gravel, silt	Mid. Pleistocene	32	Vertical	00, 253	H
10	Concud 1	Gravel, sand	Early Pleistocene	14	Vertical; Vertical	00, 126; 00, 216	A; A
11	Concud 2	Gravel, silt	Late Pliocene	38	Vertical	00, 022	VH
12	Perales	Conglomerate	Late Pliocene	10	80, 077	09, 247	A
13	Villalba Alta 1	Calc tufa	Early Pleistocene	24	Vertical	00, 284	H
14	Orrios	Gravel, sand	Mid. Pleistocene	35	Vertical	00, 175	A
15	Escorihuela	Conglomerate	Early Pleistocene	14	60, 084	30, 255	A
16	Los Baños 1	Conglomerate	Mid. Pleistocene	10	75, 010	10, 145	A
17	Los Baños 2	Conglomerate	Mid. Pleistocene	10	83, 153	00, 053	A
18	Teruel	Gravel, sand	Mid. Pleistocene	13	78, 063	12, 246	A
19	Valdecebro	Conglomerate	Late Pliocene	12	70, 250	20, 072	A
20	Fuentecerrada	Gravel	Early Pleistocene	22	70, 010	20, 191	H
21	Aldehuela	Gravel, silt	Late Pliocene	15	45, 246	45, 072	A

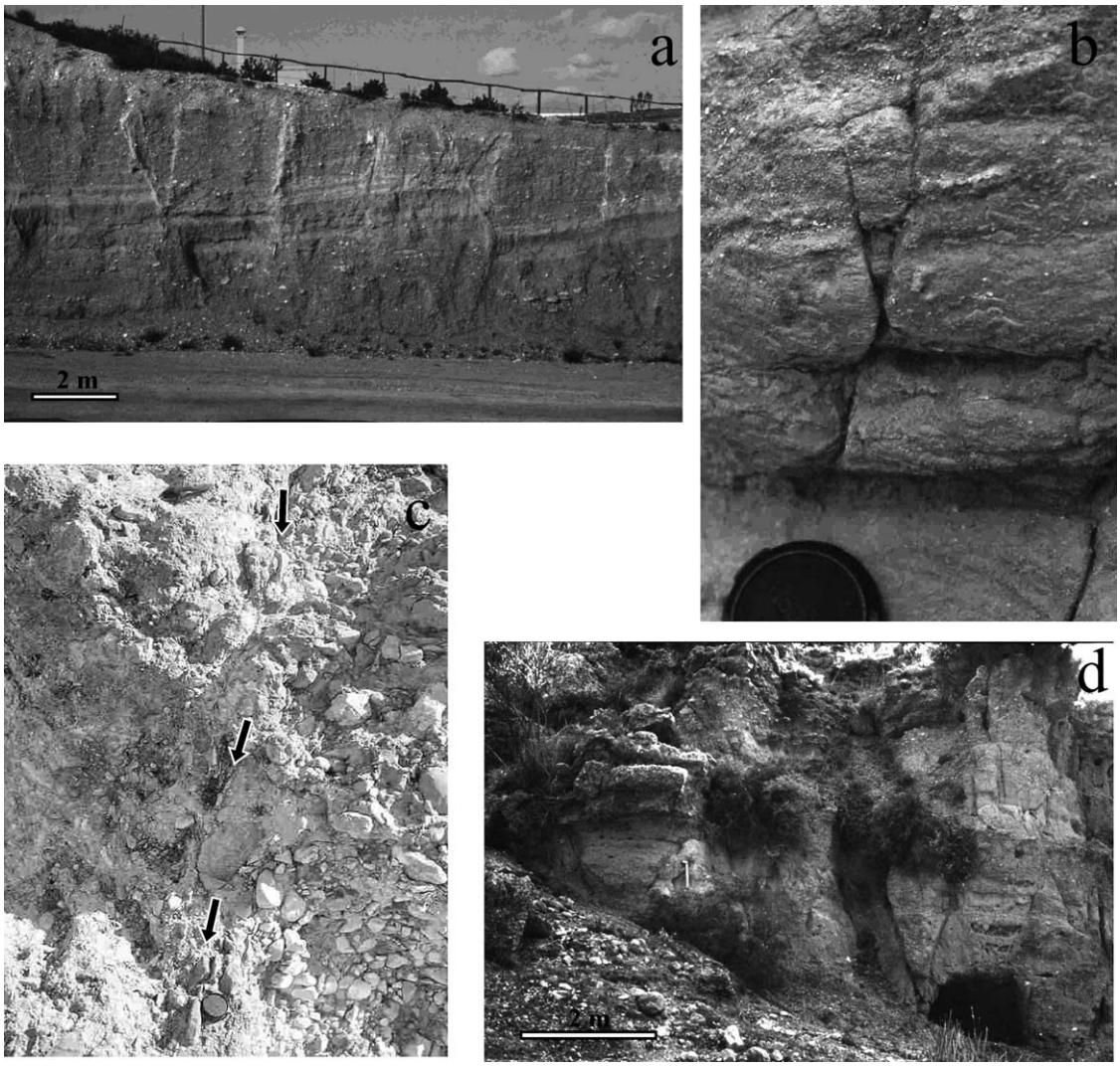

Fig. 3. Types of faults and fractures used for analysis. (a) Faults showing metric-scale offset, site 18. (b) Fractures with millimetric normal offset, site 04. (c) Brittle–ductile fracture in gravel, site 20; rotated pebbles indicate a normal shear sense. (d) Conjugate shear fractures without visible displacement, site 17.

Hancock (1985)) that could have undergone normal displacements under sufficient strain rates. The possibility of having strike-slip or reverse shear fractures can be neglected from the regional recent stress framework in the central and eastern Iberian Chain where no reverse or strike-slip fault has yet been reported in the uppermost Pliocene and Quaternary deposits.

Orientations of local palaeostress axes inferred from the fracture samples (see examples on Fig. 4) are compiled in Table 1 and Fig. 5. Most σ_1 axes are vertical or near-vertical, which is a logical result since a normal slip has been assigned to the fractures. One dominant or modal σ_3 direction usually appears in each site (two mutually orthogonal directions in sites 06, 07 and 10). These σ_3 axes are horizontal or near horizontal in most cases. The minority plunging σ_3 axes are usually parallel to dipping beds in which the fractures were collected; this suggests that the stress states predated tilting. Unfortunately, the obtained stress ratios show extremely high dispersion, so that they cannot be considered as reliable results and have not been included in Table 1. Nevertheless, most stress solutions suggest a near-multidirectional extension regime ($\sigma_2 \approx \sigma_3$), as the spectrum of compatible σ_3 axes obtained for each sample is widely distributed over the horizontal plane (Fig. 4).

The northern and central Jiloca graben shows quite consistent results. Every station shows a dominant set of mesofractures striking parallel to the neighbouring map-scale faults (NNW–SSE in the eastern margin of the graben, stations 03, 04 and 05, and NW–SE in the western margin, stations 01, 02, 06 and 07). Systematic ENE–WSW σ_3 axes are found in most sites. The two mutually orthogonal directions, N–S and E–W, obtained in sites 06 and 07 constitute the only exception. The latter are two measurement stations located very close to each other, in which Upper Pliocene and Pleistocene materials, respectively, have been surveyed. The results suggest switching of σ_2 and

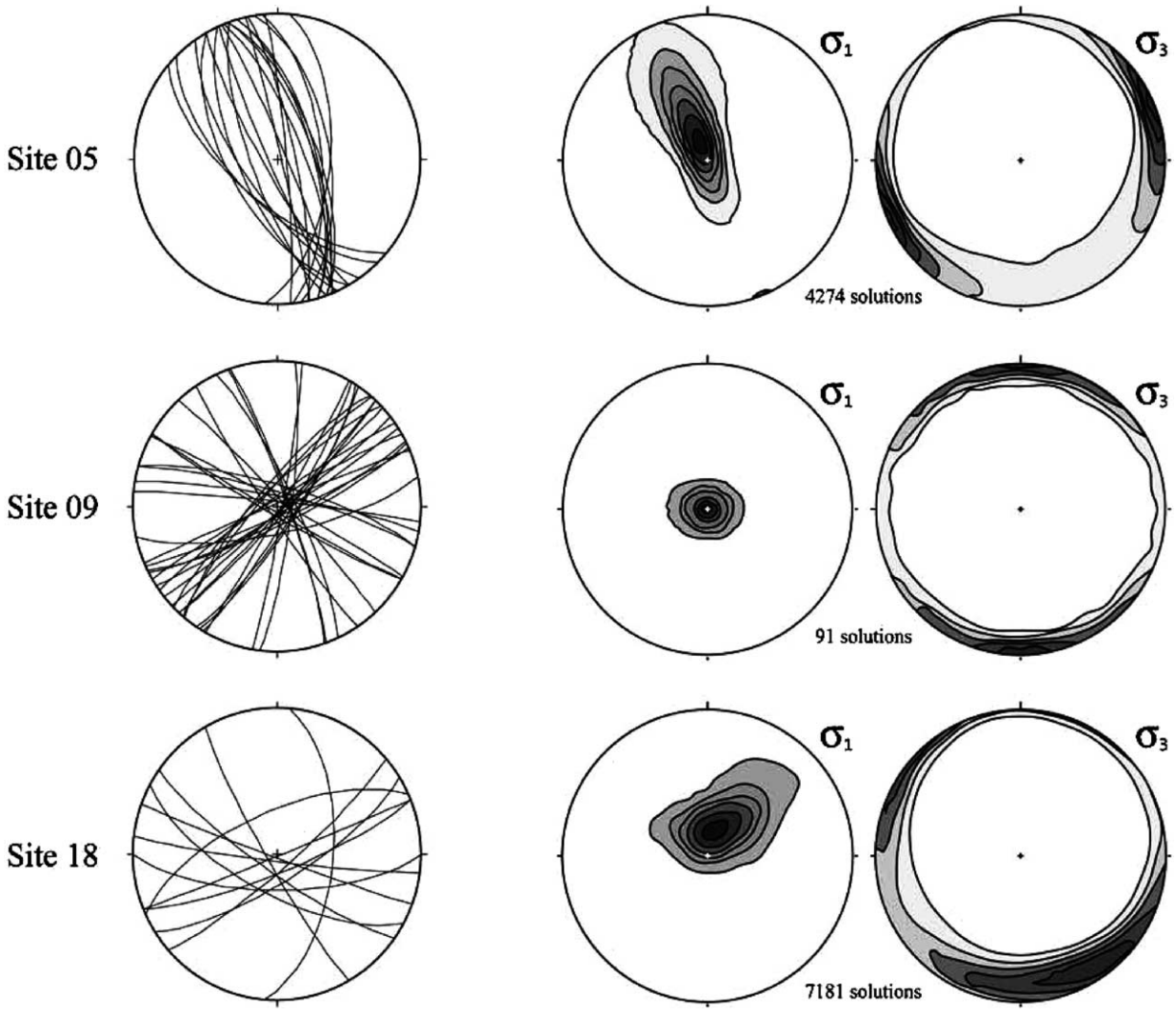

Fig. 4. Stereoplots (lower hemisphere) of fault planes from three data sites and stress inversion results (orientation of σ_1 and σ_3 axes of the ensemble of compatible stress tensors for each site).

σ_3 axes from late Pliocene to Pleistocene times at this site, though we should bear in mind the low reliability of the solution from site 06.

Mesofracture patterns in the Teruel graben show a higher dispersion. Nevertheless, ENE–WSW-trending σ_3 directions, parallel to those predominant in the Jiloca graben, are obtained in most sites (12, 15, 19, 21). The other ones trend either parallel (14) or near orthogonal (13) to the large neighbouring faults.

Finally, in the area surrounding Teruel, where the Concud fault (Jiloca graben) abuts the Teruel graben, a complex superposition of σ_3 orientations occurs. Three situations can be distinguished: (a) sites showing NW–SE to NNW–SSE mesofractures and ENE-trending σ_3 axes, similar to those inferred in the overall Jiloca and Teruel grabens (09, 18); (b) sites showing varied fracture directions but consistent NNE–SSW to NE–SW σ_3 axes approximately orthogonal to the Concud fault (08, 10, 11, 17, 20); (c) sites showing varied mesofracture directions and SE–ESE-trending σ_3 axes (approximately parallel to the Concud fault and orthogonal to the master faults of the Alfambra–Teruel segment) (10, 16).

5. Discussion and comparison with previous palaeostress interpretations

Palaeostress analysis has been carried out in the Teruel grabens by Simón (1989), Cortés and Simón (1997) and Cortés (1999) using populations of striated faults collected in Upper Miocene and Lower Pliocene lacustrine carbonates. The authors followed an analytical procedure that includes the Right Dihedra diagram (Angelier and Mechler, 1977), *y–R* diagram (Simón, 1986) and Etchecopar's method (Etchecopar et al., 1981). By compiling those numerous stress tensors (Fig. 6), the Late Neogene tectonic

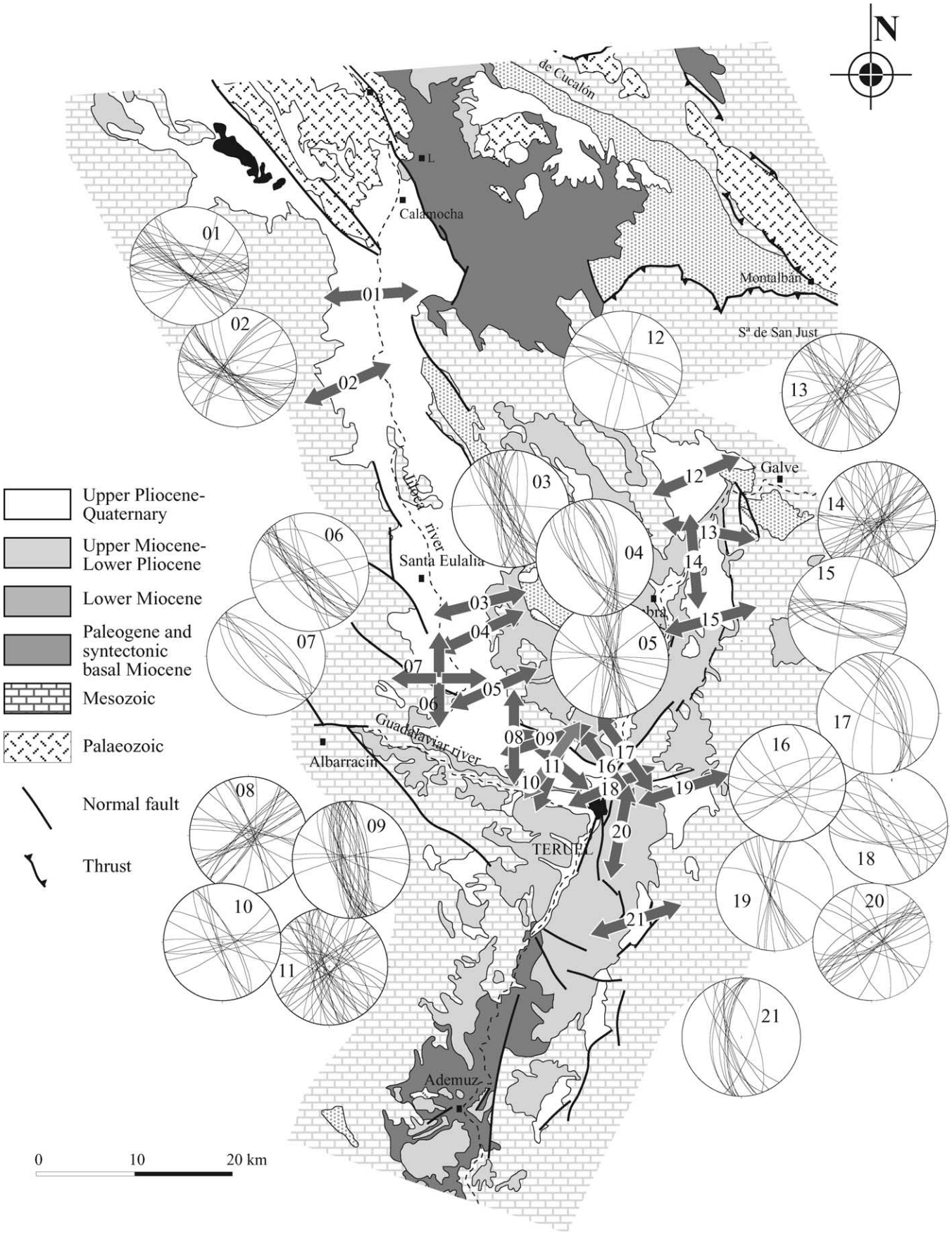
N
de Cucalón
L
Calamocha
Montalbán
Sª de San Just
Galve
Santa Eulalia
Albarracín
Guadalaviar river
Ademuz
TERUEL
0 10 20 km
Upper Pliocene-Quaternary
Upper Miocene-Lower Pliocene
Lower Miocene
Paleogene and syntectonic basal Miocene
Mesozoic
Palaeozoic
Normal fault
Thrust

evolution can be characterised as an extensional stress field with dominant E–W σ_3 trajectories, showing inhomogeneities such as deflection of stress trajectories related to large-scale faults, local switching of σ_2 and σ_3 axes and local compressional stress states. If we compare that stress field with the ensemble of results obtained in the present work we can find similarities in their essential features as well as some differences:

(a) The stress regime inferred in both cases can be defined as near-multidirectional extension ($\sigma_2 \approx \sigma_3$). This has been well established by inspecting the values of stress ratio $R=(\sigma_2-\sigma_3)/(\sigma_1-\sigma_3)$ obtained from striated fault samples (Simón, 1989; Cortés, 1999) (see Fig. 6). Looking at our results, the same interpretation is suggested by both the wide range of σ_3 trends observed in the compatible stress tensors for each individual solution (Fig. 4) and the dispersion of σ_3 trends in the ensemble of inferred stress ellipsoids (Fig. 7).

(b) The dominant σ_3 trends are close to E–W in both tensor sets (Fig. 7). Nevertheless, the modal direction is ESE–WSW in Miocene–Pliocene times (in agreement with the orientation of both the rift axis of the Valencia Trough and the onshore grabens active by that time within the central–eastern Iberian Chain) but ENE–WSW in Pliocene–Pleistocene times (agreeing with the NNW–SSE general trend of the newly developed Jiloca graben).

(c) Stress deflection caused by large-scale faults is quite significant in stress fields that affected both Miocene–Pliocene and Pliocene–Pleistocene materials. In both cases many sites show σ_3 directions near perpendicular to the neighbouring large faults (see Figs. 5 and 6). Others show σ_3 axes parallel to the latter: sites 10, 14 and 16 in Fig. 5; sites 590/04, 613/02, 612/3 and 612/4 in Fig. 6. Such types of deflection are usual at a wide range of scales in multidirectional extension stress fields. According to numerical models by Simón et al. (1988) and Kattenhorn et al. (2000), σ_3 trajectories run orthogonal to the strike of an extensional fault close to their tips, but parallel to it around its central zone. On the other hand, the occurrence of two mutually orthogonal σ_3 directions, as those inferred in sites 06, 07 and 10 of this work, may represent cases of switching of σ_2 and σ_3 axes. This phenomenon is also common in this type of stress regime. It occurs by swapping of σ_2 and σ_3 principal stresses owing to stress drop caused by the development of primary fractures, and can explain the occurrence of orthogonal joint sets (Simón et al., 1988; Rives et al., 1994; Caputo, 1995; Bai et al., 2002) as well as pairs of conjugate normal fault systems striking at right angles to each other (Simón, 1989; Angelier, 1994).

(d) Compressive stress ellipsoids were inferred only from striated faults in Upper Miocene and Lower Pliocene deposits. Some of them are coaxial with the extensional ones (both show σ_3 directions oriented close to E–W), which suggests switching of σ_1 and σ_2 axes (Simón, 1986, 1989). Such compressive and extensional stress states could coexist within a regional stress field caused by two superposed geodynamic mechanisms (Simón, 1989): (a) N–S compression caused by the convergence of Iberian and African Plates, and (b) multidirectional extension caused by crustal doming in the central–eastern Iberian Chain, related to rifting of the Valencia Trough. Other ENE- and ESE-trending σ_1 horizontal axes found by Cortés (1999) do not fit this model and suggest additional stress heterogeneities. On the contrary, no horizontal σ_1 axis has been obtained from Upper Pliocene–Pleistocene clastic materials, and no strike-slip or reverse fault was identified on them. We can interpret that the intraplate compressional component waned during the Plio-Pleistocene, in accordance with the Neogene geodynamic framework of the investigated area.

In conclusion, the extensional Late Miocene–Early Pliocene stress field essentially persists into Late Pliocene–Pleistocene times, though minor changes occur as a consequence of the geodynamic evolution.

Furthermore, a comparison can be made with the present-day stress field by considering the focal mechanisms inferred for the central–eastern Iberian Chain. An ensemble of 15 focal mechanisms, corresponding to earthquakes that occurred from 1986 to 1995, was analysed by Herraiz et al. (2000) using inversion methods proposed by Rivera and Cisternas (1990) and Giner (1996). The resulting average stress ellipsoid shows a vertical σ_1 axis, ENE–WSW-trending σ_3, and stress ratio $(\sigma_2-\sigma_3)/(\sigma_1-\sigma_3)=0.6$. The orientation of these stress axes is similar to that inferred from inversion of recent fault slip data, though the R value suggests that the extensional regime is not 'multidirectional' but 'triaxial'. The discrepancy may be a matter of depth: our fractures formed at very shallow levels (less than 30 m in all cases), whereas the hypocentres of earthquakes are located at depths from 2 to 17 km. The present-day stress field at deep levels in the crust of the Iberian Peninsula shows a primary pattern characterised by S_{Hmax} (maximum horizontal stress) trending NW–SE to N–S, directly related to plate convergence (Herraiz et al., 2000). Within this framework, the extensional stress field in the central–eastern Iberian Chain constitutes an anomaly that can be explained by isostatic loading and bending tension associated with crustal

Fig. 5. Geological map of the Teruel and Jiloca grabens and results of stress inversion in Late Pliocene–Pleistocene deposits. Stereoplots: measured fault planes. Arrows: trends of the inferred horizontal σ_3 axes (σ_1 axes are vertical or near-vertical in all cases except in site 07, where two different, not quite reliable stress solutions seem to have mixed). Data sites are labelled as in Table 1.

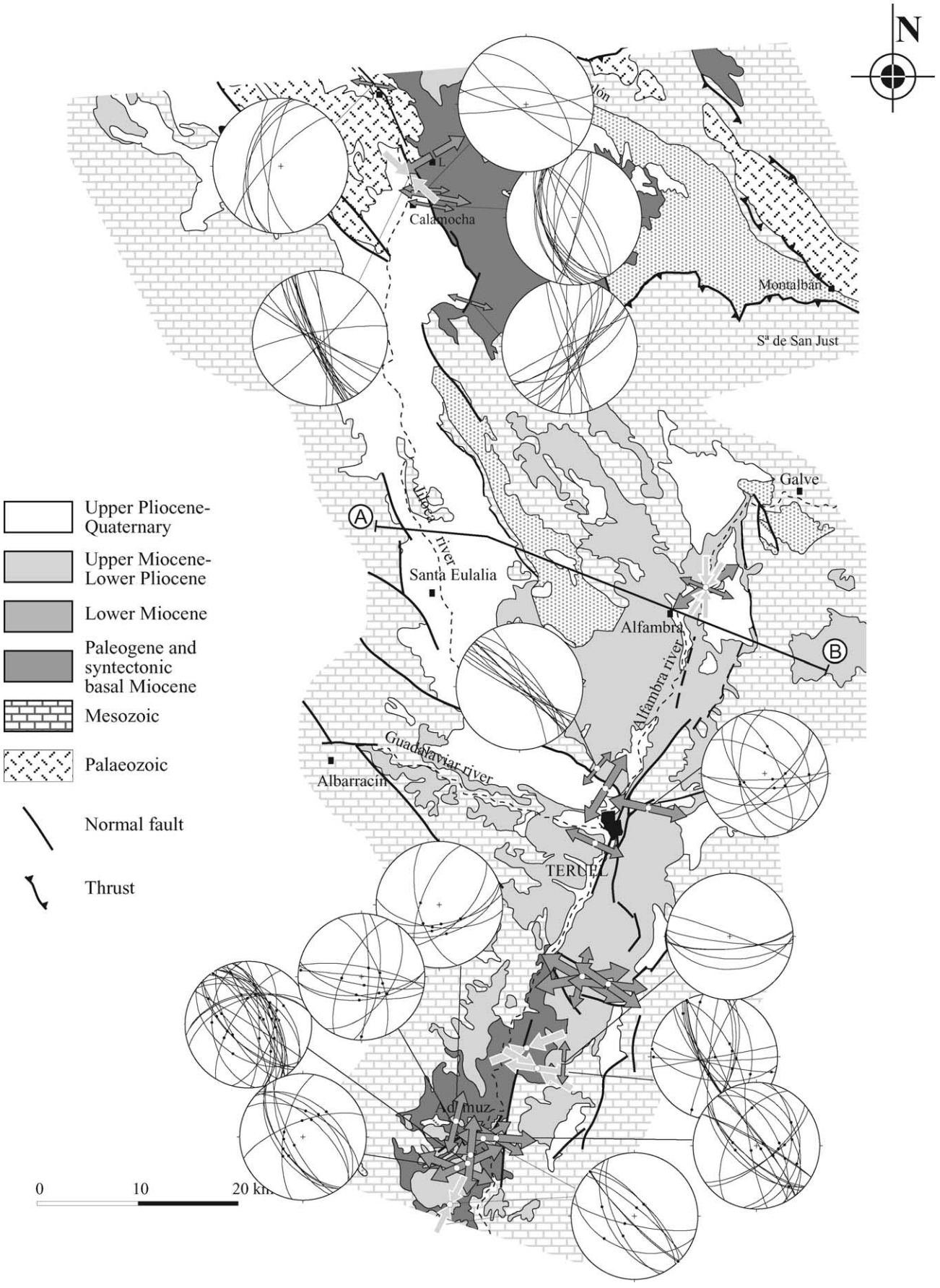
N
Calamocha
Montalbán
Sª de San Just
Galve
Santa Eulalia
Alfambra
Alfambra river
Guadalaviar river
Albarracín
TERUEL
Ad muz
A
B
Upper Pliocene-Quaternary
Upper Miocene-Lower Pliocene
Lower Miocene
Paleogene and syntectonic basal Miocene
Mesozoic
Palaeozoic
Normal fault
Thrust
0
10
20 km

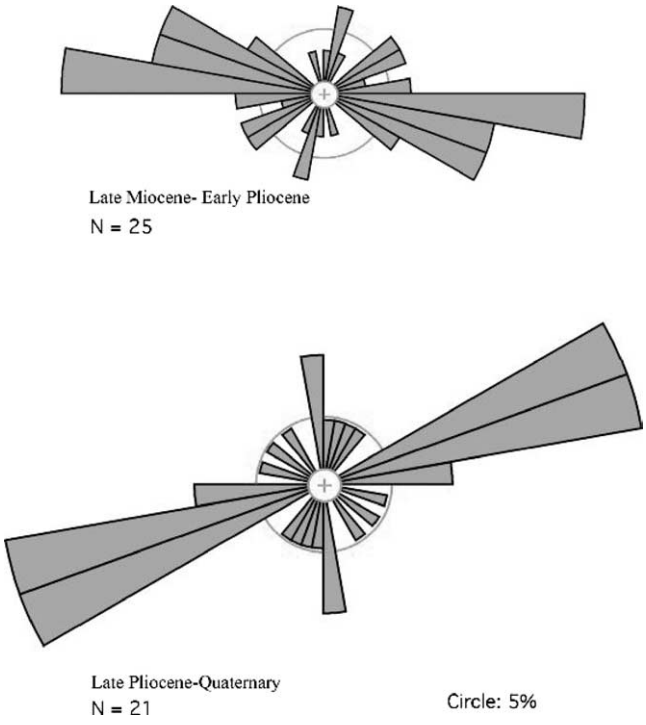

Fig. 7. Comparison of synthetic rose diagrams of σ_3 azimuths inferred from Miocene–Early Pliocene deposits (results compiled from Simón (1989) and Cortés (1999)) and late Pliocene–Pleistocene deposits (present work).

uplift at the western shoulder of the Valencia Trough. Under such a mechanism, according to theoretical models (e.g. Neugebauer and Temme, 1981; Bott, 1992; Bott and Bott, 2004), radial extension would tend to intensify upwards as approaching the outer arc of the uplift, whereas horizontal stress anisotropy induced by plate dynamics (NW–SE-trending S_{Hmax}) could remain at deeper levels.

From the methodological point of view, the regional consistency of our results gives support to the new inversion method of Lisle et al. (2001) and enhances its utility in research on recent tectonics. Stress solutions here obtained can be matched with those inferred from striated faults with respect to stress directions, although R values remain unconstrained. Nevertheless, it is true that the similarity of σ_2 and σ_3 values in the studied stress field may produce some scepticism on the reliability of the inferred σ_3 directions. A detailed analysis by Arlegui and Simón (1998) shows that, in spite of the special characteristics of the near-multidirectional extension regime, application of Etchecopar's method gives precise and reliable solutions (both in stress ratio and orientation of horizontal stress axes) from samples over 25–30 striated fault planes. This criterion, together with precision of the inferred orientations of stress axes, has been used for assessing the reliability of stress inversion results, as indicated in Table 1.

Obviously, compilation of stress ellipsoids for regional interpretation requires specification and classification of results coming from heterogeneous data or analysed by diverse procedures. Both qualitative and quantitative approaches have been proposed to assess the confidence of each individual solution within the whole set (e.g. Liesa, 2000; 'quality index' by Simón et al. (2000)). In any case, we believe that the results of the new inversion method can be combined with 'standard' stress ellipsoids inferred from striated faults in order to 'fill gaps' in our tectonic models.

6. Conclusions

The development of a new approach to stress inversion by Lisle et al. (2001) allows the fractures cutting the Upper Pliocene and Pleistocene clastic deposits in the eastern Iberian Chain to be investigated in order to reconstruct the recent stress field. The results indicate that the palaeostresses recorded in these rocks are closely related to the Late Miocene–Early Pliocene stress field, as well as to the present day stress field.

The stress field from Late Pliocene times to present day essentially represents a near-multidirectional extension regime with primary ENE–WSW-trending σ_3 trajectories, as can be inferred by comparing local palaeostress directions inferred from mesofractures with the average stress ellipsoid obtained from inversion of focal mechanisms. Moreover, those trajectories are consistent with the orientation of the most conspicuous recent macrostructure in the area (Jiloca graben). The most significant change with respect to the Miocene–Early Pliocene stress field concerns the dominant trend of σ_3 trajectories, which seems to evolve from ESE to ENE.

A poor definition of regional σ_3 trajectories is an essential feature of near-multidirectional extension because their trends are easily influenced by the previous structural setting. Large normal faults (i.e. Concud and Alfambra–Teruel segment) deflect extension trajectories to make them either orthogonal or parallel to their strikes. Switching of σ_2 and σ_3 axes (induced by local stress drop as fractures develop) represents another aspect of such stress perturbation at a smaller scale.

Acknowledgements

Dr Angel Cortés kindly granted permission to use several figures and data sets from his Ph.D. dissertation. We are very grateful to him and to Dr R. Caputo for their careful and constructive reviews. Project BTE2002-04168C03 provided funding for this research.

Fig. 6. Geological map of the Teruel and Jiloca grabens and results of stress inversion in Miocene–Early Pliocene deposits. Stereoplots: measured fault planes. Convergent arrows: trends of horizontal σ_1 axes. Divergent arrows: trends of horizontal σ_3 axes (σ_1 vertical). Arrow size reflects confidence of stress determination. Modified from Cortés (1999).

References

Adrover, R., 1986. Nuevas faunas de roedores en el Mio-Plioceno continental de la región de Teruel (España). Interés bioestratigráfico y paleoecológico. Instituto de Estudios Turolenses, Teruel.

Alcalá, L., 1994. Macromamíferos neógenos de la fosa de Alfambra–Teruel. Ph.D. thesis, University of Madrid. Publ. Instituto de Estudios Turolenses, Teruel—Museo Nacional de Ciencias Naturales, Madrid.

Alcalá, L., Alonso, A.M., Álvarez, M.A., Azanza, B., Calvo, J.P., Cañaveras, J.C., van Dam, J.A., Garcés, M., Krijgsman, W., van der Meulen, A.J., Morales, J., Peláez, P., Pérez-González, A., Sánchez, S., Sancho, R., Sanz, E., 2000. El registro sedimentario y faunístico de las cuencas de Calatayud–Daroca y Teruel. Evolución paleoambiental y paleo-climática durante el Neógeno. Revista de la Sociedad Geológica de España 13, 323–343.

Alonso, A.M., Calvo, J.P., 2000. Palustrine sedimentation in an episodically subsiding basin: the Miocene of the northern Teruel Graben (Spain). Palaeogeography, Paleoclimatology, Palaeoecology 160, 1–21.

Álvaro, M., Capote, R., Vegas, R., 1979. Un modelo de evolución geotectónica para la Cadena Celtibérica. Acta Geológica Hispánica 14, 172–177.

Amigó, J., 1986. Estructura del Massís de Gaià. Relacions estructurals amb les fosses del Penedés i del camp de Tarragona. Ph.D. thesis, University of Barcelona.

Anadón, P., Moissenet, E., 1996. Neogene basins in the Eastern Iberian Range. In: Friend, P.F., Dabrio, C.J. (Eds.), Tertiary Basins of Spain. The Stratigraphic Record of Crustal Kinematics. Cambridge University Press, Cambridge, pp. 68–76.

Angelier, J., 1991. Inversion directe de recherche 4-D: comparaison physique et mathématique de deux méthodes de détermination des tenseurs des paléocontraintes en tectonique de failles. Comptes Rendues de l'Académie des Sciences de Paris 312, 1213–1218.

Angelier, J., 1994. Fault slip analysis and paleostress reconstruction. In: Hancock, P.L. (Ed.), Continental Deformation. Pergamon Press, Oxford, pp. 53–100.

Angelier, J., Bergerat, F., 1982. Systèmes de contrainte et extension intracontinetale. Bulletin Centres de Recherche Exploration-Production Elf-Aquitaine 7, 137–147.

Angelier, J., Mechler, P., 1977. Sur une méthode graphique de recherche des contraintes principales égaleme nt utilisable en tectonique et en séismologie: la méthode des dièdres droits. Bulletin Societé géologique de France 19 (7), 1309–1318.

Arlegui, L.E., 1996. Diaclasas, fallas y campo de esfuerzos en el sector central de la cuenca del Ebro. Ph.D. thesis, University of Zaragoza.

Arlegui, L.E., Simón, J.L., 1998. Reliability of palaeostress analysis from fault striations in near multidirectional extension stress fields. Example from the Ebro Basin, Spain. Journal of Structural Geology 20, 827–840.

Armijo, R., Cisternas, A., 1978. Un problème inverse en microtectonique cassante. Comptes de l' Académie des Sciences de Paris 287, 595–598.

Armijo, R., Carey, E., Cisternas, A., 1982. The inverse problem in microtectonics and the separation of tectonic phases. Tectonophysics 82, 145–160.

Bai, T., Maerten, L., Gross, M.R., Aydin, A., 2002. Orthogonal cross joints: do they imply a regional stress rotation? Journal of Structural Geology 24, 77–88.

Bott, M.H.P., 1959. The mechanics of oblique slip faulting. Geological Magazine 96, 109–117.

Bott, M.H.P., 1992. Modelling the loading stresses associated with active continental rift systems. Tectonophysics 215, 99–115.

Bott, M.H.P., Bott, J.D.J., 2004. The Cenozoic uplift and earthquake belt of mainland Britain as a response to an underlying hot, low-density upper mantle. Journal of the Geological Society, London 161, 19–29.

Capote, R., Gutiérrez, M., Hernández, A., Olive, A., 1981. Movimientos recientes en la fosa del Jiloca (Cordillera Ibérica). V Reunión Grupo Español de Trabajo del Cuaternario, Sevilla 1981;, 245–257.

Capote, R., Muñoz, J.A., Simón, J.L., Liesa, C.L., Arlegui, L.E., 2002. Alpine tectonics I: the Alpine system north of the Betic Cordillera. In: Gibbons, W., Moreno, T. (Eds.), Geology of Spain. Geological Society, London, pp. 367–400.

Caputo, R., 1995. Evolution of orthogonal sets of coeval extension joints. Terra Nova 7, 479–490.

Carey, E., 1976. Analyse numérique d'un modèle mécanique élémentaire appliqué à l'étude d'une population de failles: calcul d'un tensor moyen des contraintes à partir des stries de glissement. Ph.D. thesis, University Paris Sud.

Carey, E., 1979. Recherche des directions principales de contraintes associées au jeu d'une population de failles. Revue de Géologie Dynamique et de Géographie Physique 21, 57–66.

Carey, E., Brunier, B., 1974. Analyse théorique et numérique d'une modèle élementaire appliqué a l'étude d'une population de failles. Comptes Rendues de l'Académie des Sciences de Paris 279, 891–894.

Casas, A.M., Cortés, A.L., 2002. Cenozoic landscape development within the central Iberian Chain, Spain. Geomorphology 44, 19–46.

Casas, A.M., Maestro, A., 1996. Deflection of a compressional stress field by large-scale basement faults. A case study from the Tertiary Almazán Basin (Spain). Tectonophysics 255, 135–156.

Casas, A.M., Simón, J.L., Serón, F.J., 1992. Stress deflection in a tectonic compressional field: a model for the northwestern Iberian Chain, Spain. Journal of Geophysical Research 97 (B5), 7183–7192.

Cortés, A.L., 1999. Evolución tectónica reciente de la Cordillera Ibérica, Cuenca del Ebro y Pirineo centro-ocidental. Ph.D. thesis, University of Zaragoza.

Cortés, A.L., Simón, J.L., 1997. Campo de esfuerzos recientes en la fosa de Alfambra-Teruel-Mira. In: Calvo, J.P., Morales, J. (Eds.), Avances en el conocimiento del Terciario Ibérico. Universidad Complutense de Madrid-CSIC, Madrid, pp. 65–68.

Delvaux, D., 1994. Tensor Interactive MS-DOS Quick Basic Program Developed for Paleostress Determinations on Geological Fractures and Earthquake Focal Mechanisms. Royal Museum for Central Africa, Tervuren.

Delvaux, D., Levi, K., Kajara, R., Sarota, J., 1992. Cenozoic paleostress and kinematic evolution of the Rukwa–North Malawi rift valley (East African Rift System). Bulletin Centres de Recherche Exploration-Production Elf-Aquitaine 16, 383–406.

Etchecopar, A., 1984. Etude des états de contraintes en tectonique cassante et simulations de déformations plastiques (approche mathématique). Ph.D. thesis, USTL Montpellier.

Etchecopar, A., Vasseur, G., Daignières, M., 1981. An inverse problem in microtectonics for the determination of stress tensors from fault striation analysis. Journal of Structural Geology 3, 51–65.

Fry, N., 1992. Stress ratio determinations from striated faults: a spherical plot for cases of near-vertical principal stress. Journal of Structural Geology 14, 1121–1131.

Giner, J.L., 1996. Análisis neotectónico y sismotectónico en la parte centro-oriental de la cuenca del Tajo. Ph.D. thesis, University of Madrid.

Gracia, F.J., Gutiérrez, F., Gutiérrez, M., 2003. The Jiloca karst polje-tectonic graben (Iberian Range, NE Spain). Geomorphology 52, 215–231.

Gracia, F.J., Gutiérrez, M., Leránoz, B., 1988. Las superficies de erosion neógenas en el sector central de la Cordillera Ibérica. Revista de la Sociedad Geológica de España 1, 135–142.

Guimerà, J., 1988. Estudi estructural de l'enllaç entre la Serralada Iberica y la Serralada Costanera Catalana. Ph.D. thesis, University of Barcelona.

Gutiérrez, F., Gracia, F.J., Gutiérrez, M., 1996. Consideraciones sobre el final del relleno endorreico de las fosas de Calatayud y Teruel y su paso al exorreísmo. Implicaciones morfo-estratigráficas y estructurales. In: Grandal, A., Pagés, J. (Eds.), IV Reunión de Geomorfología. Sociedad Española de Geomorfología, O Castro (A Coruña), pp. 23–43.

Hancock, P.L., 1985. Brittle microtectonics: principles and practice. Journal of Structural Geology 7, 437–457.

Herraiz, M., De Vicente, G., Lindo-Ñaupari, R., Giner, J., Simón, J.L., González-Casado, J.M., Vadillo, O., Rodríguez-Pascua, M.A.,

Cicuéndez, J.I., Casas, A., Cabañas, L., Rincón, P., Cortés, A.L., Ramírez, M., Lucini, M., 2000. The recent (upper Miocene to Quaternary) and present tectonic stress distributions in the Iberian Peninsula. Tectonics 19, 762–786.

IGME (Ed.), 1983. Mapa Geológico de España 1:50,000, Hoja 567 (Teruel). I.G.M.E., Madrid.

Kattenhorn, S.A., Aydin, A., Pollard, D.D., 2000. Joints at high angles to normal fault strike: an explanation using 3-D numerical models of fault-perturbed stress fields. Journal of Structural Geology 22, 1–23.

Liesa, C.L., 2000. Fracturación y campos de esfuerzos compresivos alpinos en la Cordillera Ibérica y el NE peninsular. Ph.D. thesis, University of Zaragoza.

Lisle, R.J., 1987. Principal stress orientations from faults: an additional constraint. Annales Tectonicae 1, 155–158.

Lisle, R.J., 1988. Romsa: a Basic program for paleostress analysis using fault striation data. Computers & Geoscience 14, 255–259.

Lisle, R.J., Orife, T., Arlegui, L.E., 2001. A stress inversion method requiring only fault slip sense. Journal of Geophysical Research 106 (B2), 2281–2289.

Moissenet, E., 1982. Le Villafranchien de la Région de Teruel (Espagne). Stratigraphie-Deformations-Milieux. Collòque Le Villafranchien Méditerranéen, Lille, pp. 229–253.

Moissenet, E., 1983. Aspectos de la neotectónica en la fosa de Teruel. In: Comba, J.A. (Ed.), Geología de España. Libro Jubilar J.M. Ríos, I.G.M.E., Madrid, pp. 427–446.

Moissenet, E., 1985. Le Quaternaire moyen alluvial du fossé de Teruel (Espagne). Physio-Géo. 14/15, 61–78.

Neugebauer, H.J., Temme, P., 1981. Crustal uplift and the propagation of failure zones. Tectonophysics 73, 33–51.

Orife, T., Arlegui, L.E., Lisle, R.J., 2002. Dipslip: a QuickBasic stress inversion program for analyzing sets of faults without slip lineations. Computers & Geosciences 28, 775–781.

Pegoraro, O., 1972. Application de la microtectonique à un étude de neotectonique. Le golfe Maliaque (Grèce centrale). Ph.D. thesis, USTL Montpellier.

Riba, O., 1959. Estudio Geológico de la Sierra de Albarracín. Instituto Lucas Mallada, C.S.I.C., Madrid.

Rivera, L.A., Cisternas, A., 1990. Stress tensor and fault plane solutions for a population of earthquakes. Bulletin Seismological Society of America 80, 600–614.

Rives, T., Rawnsley, K.D., Petit, J.P., 1994. Analogue simulation of natural orthogonal joint set formation in brittle varnish. Journal of Structural Geology 16, 419–429.

Roca, E., Guimerà, J., 1992. The Neogene structure of the eastern Iberian margin: structural constraints on the crustal evolution of the Valencia trough (western Mediterranean). Tectonophysics 203, 203–218.

Rubio, J.C., 2004. Los humedales del Alto Jiloca: estudio hidrogeológico e histórico-arqueológico. Ph.D. thesis, University of Zaragoza.

Simón, J.L., 1982. Compresión y distensión alpinas en la Cadena Ibérica Oriental. Tesis Doct. Universidad de Zaragoza. Ph.D. thesis, University of Zaragoza. Publ. Instituto de Estudios Turolenses, Teruel (1984).

Simón, J.L., 1983. Tectónica y neotectónica del sistema de fosas de Teruel. Teruel 69, 21–97.

Simón, J.L., 1986. Analysis of a gradual change in stress regime (example from the eastern Iberian Chain, Spain). Tectonophysics 124, 37–53.

Simón, J.L., 1989. Late Cenozoic stress field and fracturing in the Iberian Chain and Ebro Basin (Spain). Journal of Structural Geology 11, 285–294.

Simón, J.L., Soriano, M.A., 1993. La falla de Concud (Teruel): actividad cuaternaria y régimen de esfuerzos asociado. In: Aleixandre, T., Pérez González, A. (Eds.), El Cuaternario de España y Portugal. Instituto Tecnológico GeoMinero de España, Madrid, pp. 729–737.

Simón, J.L., Serón, F.J., Casas, A.M., 1988. Stress deflection and fracture development in a multidirectional extension regime. Mathematical and experimental approach with field examples. Annales Tectonicae 2, 21–32.

Simón, J.L., Arlegui, L.E., Cortés, A.L., Maestro, A., 2000. Evaluación de la calidad de los tensores de esfuerzos: el índice IQ. Geotemas 1, 83–86.

Stapel, G., Moeys, R.P., 1994. Manual for the D. Delvaux Tensor program. In: Moeys, R.P., Stapel, G. (Eds.), Paleostress Evolution in the Altai and Baikal Regions, South Siberia. Internal Report Free University, Amsterdam, pp. 3–28.

Vegas, R., Fontboté, J.M., Banda, E., 1979. Widespread Neogene rifting superimposed on alpine regions of the Iberian Peninsula. Proceedings Symposium Evolution and Tectonics of the Western Mediterranean and Surrounding Areas, EGS, Vienna. Instituto Geográfico Nacional, Madrid, Special Publication 201, pp. 109–128.